The Relationship Between

Patterns of Benthic Fauna and Zooplankton in the Chukchi Sea and Physical Forcing

By Maria N. Pisareva, Robert S. Pickart, Katrin Iken, Elizaveta A. Ershova, Jacqueline M. Grebmeier, Lee W. Cooper, Bodil A. Bluhm, Carolina Nobre, Russell R. Hopcroft, Haoguo Hu, Jia Wang, Carin J. Ashjian, Ksenia N. Kosobokova, and Terry E. Whitledge

Photo credit: Aleksey Ostrovskiy

ABSTRACT. Using data from a number of summer surveys of the Chukchi Sea over the past decade, we investigate aspects in which the benthic fauna, sediment structure, and zooplankton there are related to circulation patterns and shelf hydrographic conditions. A flow speed map is constructed that reveals the major pathways on the shelf. Regions of enhanced flow speed are dictated by lateral constrictions—in particular, Bering Strait and Barrow and Herald Canyons—and by sloping topography near coastlines. For the most part, benthic epifaunal and macrofaunal suspension feeders are found in high flow regimes, while deposit feeders are located in regions of weaker flow. The major exceptions are in Bering Strait, where benthic sampling was underrepresented, and in Herald Canyon where the pattern is inexplicably reversed. Sediment grain size is also largely consistent with variations in flow speed on the shelf. Data from three biophysical surveys of the Chukchi Sea, carried out as part of the Russian-American Long-term Census of the Arctic program, reveal close relationships between the water masses and the zooplankton communities on the shelf. Variations in atmospheric forcing, particularly wind, during the three sampling periods caused significant changes in the lateral and vertical distributions of the summer and winter water masses. These water mass changes, in turn, were reflected in the amounts and species of zooplankton observed throughout the shelf in each survey. Our study highlights the close relationship between physical drivers (wind forcing, water masses, circulation, and sediment type) in the Chukchi Sea and the biological signals in the benthos and the plankton on a variety of time scales.

INTRODUCTION

Seasonally varying waters of Pacific origin profoundly influence the ecosystem of the western Arctic Ocean. Pacific summer water is one of the primary sources of freshwater to the Arctic (Woodgate et al., 2012) and contributes to ice melt in the interior basin (Steele et al., 2010). Pacific Winter Water ventilates the interior halocline (Pickart et al., 2005) and is a major source of nutrients that spur primary production in the region (Lowry et al., 2015). Atmospheric forcing, sea ice, and topography significantly modify the waters as they advect northward through Bering Strait across the wide and shallow Chukchi Sea shelf. The water masses on the shelf have been strongly impacted by loss of sea ice, increased winds, and enhanced solar heating resulting from recent and rapid environmental change at high latitudes (Wood et al., 2015, in this issue; Woodgate et al., 2015, in this issue). Hence, to improve our understanding of how the western Arctic ecosystem functions and how it will respond to the changing physical drivers, it is important to study the coupled physical-biological processes on the Chukchi shelf where the water first enters the Arctic domain.

Three main pathways of Pacific-origin waters heading toward the Arctic Basin are believed to exist in the Chukchi Sea (Figure 1a). A narrow, surface-intensified flow of warm Alaskan Coastal Water, originating from river runoff in the Gulf of Alaska, follows the Alaskan coast northward to Barrow Canyon in summer (Paquette and Bourke, 1974). The water emanating from the central and western Bering Sea divides into two branches north of Bering Strait. One branch progresses through the Central Channel (Weingartner et al., 2005) and is diverted eastward into Barrow Canyon. The second branch veers to the northwest and flows through Herald Canyon. In summertime, this water is a mixture of moderately warm Bering Shelf Water and Anadyr Water (Coachman et al., 1975), and in winter it is transformed by convective overturning that lowers the temperature to near the freezing point. The Pacific Winter Water can be further modified within polynyas on the Chukchi shelf (e.g., Weingartner et al., 1998; Itoh et al., 2015). Presently, it is unknown to what degree this Pacific Winter Water is fluxed northward within the coastal branch adjacent to Alaska.

In addition to Pacific-origin waters on the Chukchi shelf, there are water masses of local Arctic origin. Fresh and typically cold Siberian Coastal Water originates from river runoff in the western East Siberian Sea, including discharge from the Lena River, and inflow of Laptev Sea water (Weingartner et al., 1999). This water flows southeastward in the quasi-permanent Siberian Coastal Current, which is strongly influenced by wind (Weingartner et al., 1999). Before reaching Bering Strait, the current is believed to veer offshore and mix with ambient waters. The other local water mass on the Chukchi shelf is near-surface ice meltwater that is prevalent in late spring into summer.

While the advection of seasonally varying waters is known to influence biogeochemical processes and ecosystem function in the Chukchi Sea (e.g., Grebmeier et al., 2015a), many questions remain regarding how the hydrographic conditions and circulation on the shelf impact biological composition in the water column and the benthos. Furthermore, it may be that various biological metrics could inform us about aspects of the physical forcing, especially in light of the large mesoscale variability on the shelf. In this study, we use multiple physical and biological data sets to address relationships between the physical drivers—in particular, wind forcing, water masses, circulation, and sediment type—and species distribution and function of benthic fauna and zooplankton. We assess these physical-biological connections on two sets of time scales. The benthic invertebrate system integrates water column processes such as flow regimes and productivity on time scales of many years to decades because of the typically long life spans and the limited mobility of these organisms. This topic is addressed in the first part of the paper. In contrast, zooplankton in the pelagic system respond on the order of weeks to months to changes in physical forcing, affording us the opportunity to investigate the connection between environmental factors

and biological signals in the water column on a survey-to-survey basis. This topic is addressed in the second part of the paper.

The primary data used in our study come from three broad-scale biophysical surveys of the Chukchi Sea conducted in 2004, 2009, and 2012 as part of the Russian-American Long-term Census of the Arctic (RUSALCA) program. These surveys are augmented with data from other parts of the shelf collected over the past decade. Together, the observations converge to describe a system that is heavily dependent on advection, with persistent patterns formed by the pathways and speeds of the currents on both long and short temporal scales.

DATA AND METHODS
Observations

Three biophysical surveys in 2004 (August 10–22), 2009 (September 6–29), and 2012 (August 30–September 16) were undertaken in the Chukchi Sea as a part of the RUSALCA program (Figure 1b–d). The sampling pattern included transects in the southern part of the sea, the region around Wrangel Island, and in Herald Canyon. Some of the transects were repeat occupations over the different years in order to facilitate the detection of interannual patterns. Notably, the Chukchi South (CS) line, from Point Hope, Alaska, to Serdtse-Kamen', Russia, coincides with the Distributed Biological Observatory (DBO) transect 3 (see Grebmeier et al., 2010, and http://www. arctic.noaa.gov/dbo). This transect, however, is limited during most surveys to the
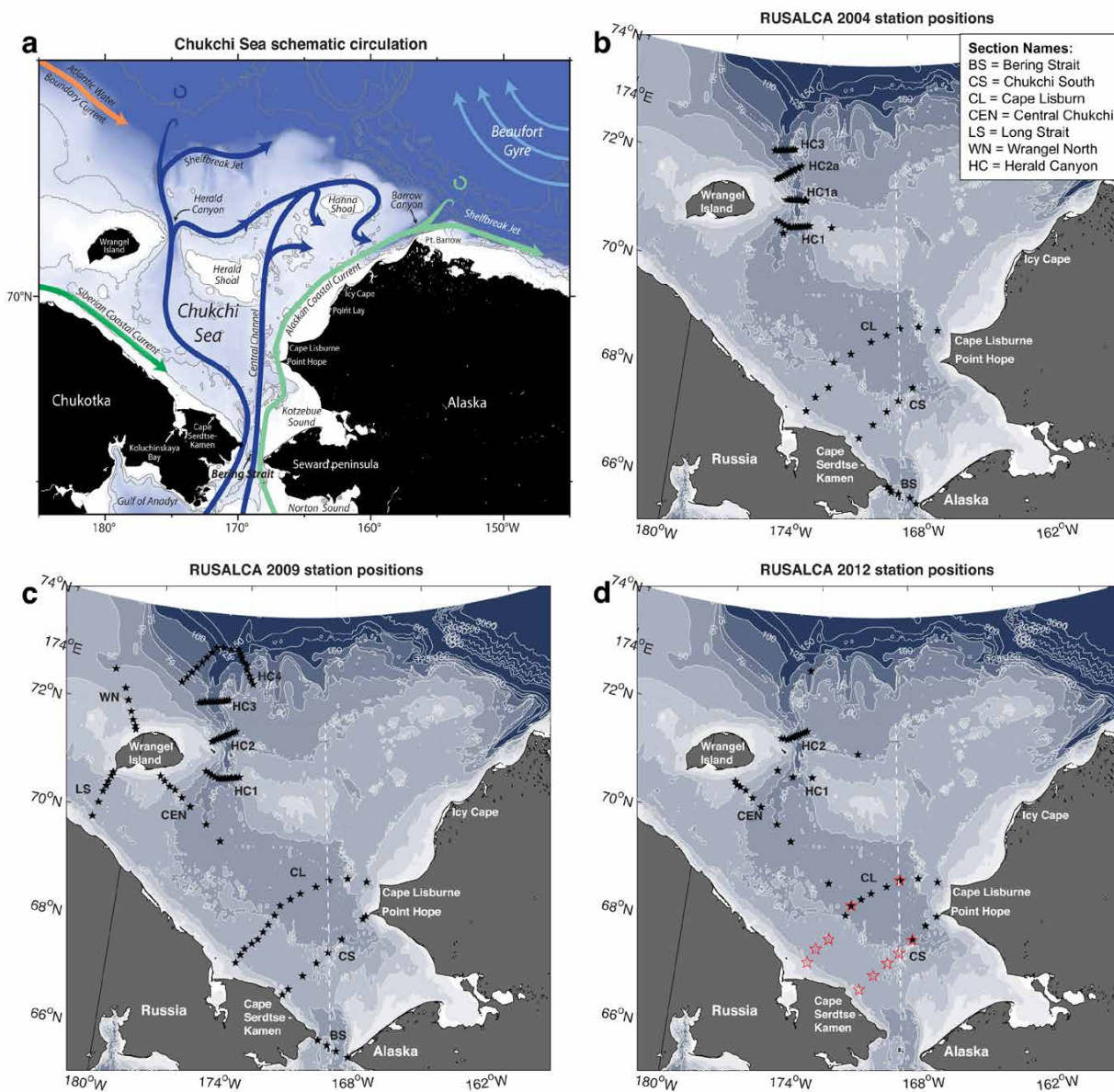

FIGURE 1. Schematic circulation of the Chukchi Sea (after Brugler et al., 2014) with place names (a) and hydrographic stations occupied during the (b) 2004, (c) 2009, and (d) 2012 RUSALCA cruises. See the legend for the names of the transects. The red stars indicate second occupations of the same transect lines. The white dashed line denotes the Russian–US convention line, and the solid white contours are the bottom depth.

eastern portion within the United States Exclusive Economic Zone and does not completely cover the region of enhanced biological activity. The capability of the RUSALCA program to sample across the international boundary is one of the key strengths of the program.

A large number of physical and biological parameters were measured both in the water column and at the seafloor during the cruises. In this study, we use conductivity-temperature-depth (CTD) data, velocity profiles from a lowered acoustic Doppler current profiler (LADCP), nutrient data, vertical zooplankton net tow and video plankton recorder data, benthic macrofauna data from bottom grabs, and epifauna data from trawls. In addition to the measurements collected during the RUSALCA program, we make use of historical or other contemporary data from the Chukchi shelf drawn from a number of additional programs.

Hydrography and Nutrients

The CTD data were collected using a Sea-Bird 911+ instrument, and the LADCP system that consisted of an upward- and downward-facing 300 KHz RDI Workhorse pair. These instruments were mounted on a rosette with Niskin bottles whose samples were analyzed for nutrients (nitrite, nitrate, ammonium, silicate, phosphate) at six to eight different depths through the water column (Yun et al., 2014). In each case, the CTD was pre- and post-cruise calibrated, and the nutrient samples were either processed onboard using an automated nutrient analyzer (ALPKEM RFA model 300) following Whitledge et al. (1981) or frozen for processing ashore. For more information on the CTD and LADCP data collection and processing, including sensor accuracies, refer to Pickart et al. (2010), Pisareva et al. (2015), and the three cruise reports (http://www.whoi.edu/science/PO/people/pickart/newFieldPrograms.htm).

The RUSALCA physical oceanographic data were supplemented with shipboard ADCP data from the eastern Chukchi

Sea and the Chukotka region collected on various cruises aboard USCGC *Healy*, R/V *Nathaniel B. Palmer*, and R/V *Alpha Helix* in the early 1990s and in 2003, 2010, 2011, and 2014. All of the data are confined to the months of June to October. A map of flow speed on the Chukchi shelf was constructed as follows. First, using the atmospheric fields from the North American Regional Reanalysis (see later section on Atmospheric Reanalysis Fields and Satellite Data), we removed all of the ADCP velocity profiles that were obtained when the wind speed exceeded 10 m s^{-1} for any six-hour period during the day of the measurement at the given location. Winds of this magnitude have been shown to disrupt normal flow patterns on the Chukchi shelf (e.g., Pickart et al., 2011; results were not sensitive to the precise choice of cutoff used). We also removed instances when the Alaskan Coastal Current was reversed (i.e., flowing to the south). Both of these measures were implemented to remove anomalous data points, and indeed the resulting flow speed map became more interpretable. The depth-averaged flow speed was then computed using the remaining data and subsequently interpolated laterally onto a 0.2° latitude by 0.5° longitude grid using a Laplacian-Spline routine (e.g., Pickart et al., 2010). Finally, the flow speed was smoothed using a Laplacian filter to reduce high wavenumber noise.

Benthic Fauna

For the investigation of feeding types of epifauna and macrofauna, we used data collected in the Chukchi Sea from multiple studies during the last decade, including RUSALCA, the Western Arctic Shelf-basin Interactions program, the Arctic Ecosystem Integrated Survey, and the Chukchi Sea Offshore Monitoring in Drilling Area (Chemical and Benthos) Hanna Shoal project (Dunton, 2015; Grebmeier et al., 2015a). Biomass data for both epifauna and macrofauna were averaged on a grid of 1° longitude by 0.4° degree latitude. For a description of the macrofauna sampling protocol, see

Grebmeier et al. (2015a) and Grebmeier et al. (2015b, in this issue). Epifauna samples were collected following the procedure described in Bluhm et al. (2009) and Ravelo et al. (2014). For each station, we divided the macrofauna and epifauna species into several feeding type categories, specifically: deposit feeders, suspension feeders, and others (for species that did not fall into the former two categories), using our own knowledge and published data in MacDonald et al. (2010), Appeltans et al. (2012), and references in Denisenko et al. (2015, in this issue). We then calculated the biomass percentage of suspension feeders versus deposit feeders for both macrofauna and epifauna within a composite grab or trawl station using only the combination of the two feeding types as the total biomass for the calculation.

Sediment Grain Size

Surface sediment subsamples (0–1 cm) were collected during the RUSALCA cruises from a single 0.1 m² van Veen grab, packaged in Whirl-Pak bags, and frozen for post-cruise grain size determinations as well as organic carbon and nitrogen content following standard sampling methods (Cooper et al., 1998; Grebmeier, 2012). Additional data used in the study come from Grebmeier and Cooper (2014). Further details of the methods can be found in Cooper et al. (2015, in this issue), who carried out an extensive investigation of sediment grain size distributions in the Chukchi Sea.

Zooplankton

Zooplankton vertical net tows were conducted during the three RUSALCA cruises using a 150 μm double ring net with 60 cm mouth diameters. Each of the tows provided zooplankton samples that integrated the full water column. In addition, large and rare taxa were collected in 2009 and 2012 with 505 μm Bongo nets that were towed obliquely behind the ship to a depth near the bottom (Ershova et al., 2015). Cluster analysis was used to identify co-occurring groups of zooplankton

species and taxa that were associated with different water masses. For a detailed discussion of the sampling, preservation, and processing of the zooplankton data, see Ershova et al. (2015). A self-contained, battery-powered, single camera Auto Video Plankton Recorder (AVPR, SeaScan, Inc.) was used to describe the distributions and abundance of taxa and particles. The AVPR was mounted in the CTD rosette and hence obtained profiles from the surface to near bottom. Only the downcast data were used to ensure that the images sampled undisturbed water. In-focus images were extracted and identified using the automated focus detection (AutoDeck) program (SeaScan Inc.) and the Visual Plankton identification program developed at the Woods Hole Oceanographic Institution (Davis et al., 1996, 2004; Tang et al, 1998; Hu and Davis, 2005). The automatic identifications were verified manually using Visual Plankton. For details of the AVPR processing, see Ashjian et al. (2005).

Atmospheric Reanalysis Fields and Satellite Data

The North American Regional Reanalysis (NARR, Mesinger, 2006) sea level pressure data and 10 m winds were used to investigate the atmospheric conditions in the region during the three RUSALCA surveys. The spatial resolution of the data is 32 km and the temporal resolution is six hours. To characterize sea ice concentration and sea surface temperature (SST), we use the blended Advanced Very High Resolution Radiometer (AVHRR) and the Advanced Microwave Scanning Radiometer (AMSR) product (see Reynolds et al., 2007). The spatial resolution of these fields is 0.25°, and the temporal resolution is once per day. The accuracy of the sea ice concentration data is estimated to be ±10% (Cavalieri et al., 1991).

Numerical Model Fields

A depth-averaged flow speed map was constructed using output from the Sea Ice Ocean Model (Wang et al., 2014) for comparison with the map made from the in situ observations. The time period considered in the model was summer (June–September) 2009, and the model data were interpolated onto the same grid used for the observations. The Sea Ice Ocean Model uses the Princeton Ocean Model (POM; Blumberg and Mellor, 1987; Mellor, 2004) and the full thermodynamic-dynamic ice model of Hibler (1979). The zonal resolution ranges from ~5 km near the northern boundary to ~9 km near the Aleutian Islands, and the meridional resolution is the same throughout the domain, ~9 km. This spacing is smaller than the internal deformation radius in the Canadian sector of the Arctic Ocean (13 km) as estimated by Zhao et al. (2014). There are 24 sigma levels, with higher vertical resolution near the surface and the bottom for a more accurate representation of surface and bottom boundary layer processes. The model was initialized with climatological temperature and salinity data from the Polar Science Center Hydrographic Climatology (PHC 3.0, Steele et al., 2001). The atmospheric forcing fields are taken from the National Centers for Environmental Prediction (NCEP) six-hourly reanalysis data.

FLOW SPEED PATTERNS AND THEIR IMPACTS
Observational Flow Speed Map

We begin by presenting the map of depth-integrated flow speed in the Chukchi Sea derived from various shipboard ADCP data collected during the last decade (Figure 2a). Not surprisingly, some of the features differ from the schematic circulation depicted in Figure 1a due to the high temporal variability of the hydrography and flow on the shelf and its dependence on a number of physical drivers (e.g., Winsor and Chapman, 2004; Woodgate et al., 2005). Furthermore, recent evidence suggests that the circulation in the Northeast Chukchi Sea (at least in summertime) is more complex than previously thought (Weingartner et al., 2013; Pickart et al., in press). Nonetheless, clear patterns are evident in Figure 2a that are in line with what is known about the flow on the shelf.

The enhanced depth-integrated flows through the lateral constrictions of Bering Strait, Barrow Canyon, and the eastern flank of Herald Canyon (e.g., Woodgate et al., 2012; Münchow and Carmack, 1997; Pickart et al., 2010; Pisareva et al., 2015) are all evident in Figure 2a. The Central Channel pathway (Weingartner et al., 2005), including the extension that advects Pacific water anticyclonically around the north side of Hanna Shoal (Winsor and Chapman, 2004; Spall, 2007), is also evident, although it is somewhat patchy. This patchiness likely reflects the generally weak flow speeds along this branch (Weingartner et al., 2005) and its sensitivity to wind forcing (e.g., Pickart et al., 2011). The Siberian Coastal Current (SCC), which flows southeastward along the coast of Chukotka toward Bering Strait is apparent as well in our flow speed map, but, again, it is patchy. Although the SCC is a buoyancy-driven current (Weingartner et al., 1999), it is highly sensitive to the coastal wind field, which likely explains the variable nature of this feature in Figure 2a.

Notably, the Alaskan Coastal Current (ACC) has no consistent signature in the flow speed map. Adjacent to the Alaska coast, the speed alternates between regions of stronger and weaker values. In particular, northeast of Bering Strait—along the eastern portion of the Seward Peninsula and offshore of Kotzebue Sound—the flow speed is relatively weak. North of there, the speed increases again to the region of Cape Lisburne, and farther north it once again slows until roughly Icy Cape, after which it increases into Barrow Canyon. This spatial variability can be largely explained by variations in topography. To first order, the ACC follows the isobaths adjacent to the coast. Assuming the transport of the current stays the same, its velocity will be enhanced where the isobaths are tightly spaced (large bottom slope) and weaker where the isobaths are spaced farther apart (weaker bottom slope). Using the ETOPO2 bathymetry, we created a map

of the bottom slope on the Chukchi shelf (Figure 2b) by gridding the bottom depth at a coarser resolution (10 km grid versus the 3.7 km of ETOPO2), smoothing it multiple times with a Laplacian filter, then computing the gradient (the general patterns are not sensitive to the precise gridding and smoothing).

There is good correspondence between the variation in ACC flow speed and the magnitude of the bottom slope adjacent to the Alaskan coast (compare Figure 2a and 2b). In particular, the largest flow speeds and bottom slopes are found between Kotzebue Sound and Cape Lisburne, and again from approximately Icy Cape into Barrow Canyon. The bottom slopes are also large adjacent to the Siberian coast, corresponding to the strong flow of the SCC. Lastly, approaching the southeastern end of Herald Canyon, the topographic slope increases as does the flow speed.

Model Flow Speed Map

We now compare the observed pattern of flow speeds on the Chukchi shelf with that obtained from the Sea Ice Ocean Model for the summer months of 2009 (the observational map is also based on summertime data). Overall, the agreement between the model and the data is impressive (compare Figure 2a and 2c). As was true for the observations, the model shows enhanced flow speeds in Bering Strait, Barrow Canyon, and on the eastern side of Herald Canyon. The Central Channel pathway that extends around the north side Hanna Shoal is also present in the model, but, similar to the observations, this pathway is somewhat patchy. Notably, the model ACC alternates between weaker and stronger flow in generally the same regions as seen in the observations, consistent with the varying bottom slope along the current's path from Bering Strait to Barrow Canyon. The main disagreement between the model and the observations is that the model does not show a strong SCC, possibly due to the significant seasonal to interannual variability of the current (Weingartner et al., 1999). The main conclusion from the two maps is that enhanced flow speeds are dictated by two main factors: lateral constrictions and the varying bottom slope along the path of the ACC. Next, we explore the relationship between the flow speeds on the shelf and various biological and chemical signals.

Relation to Benthic Fauna

It has been suggested that the feeding mode of benthic fauna is related to the strength of the currents on the shelf (Feder et al., 1994, 2007; Grebmeier et al., 2006; Blanchard et al., 2013). In particular, suspension feeders (e.g., corals, anemones,

FIGURE 2. (a) Depth-averaged flow speed for the summer months from the observational data (color, cm s⁻¹). The gray circles indicate the data points. (b) Map of the bathymetric gradient (color). (c) Depth-averaged flow speed for June to September 2009 from the numerical model (color, cm s⁻¹). The gray and black contours indicate bottom depth.
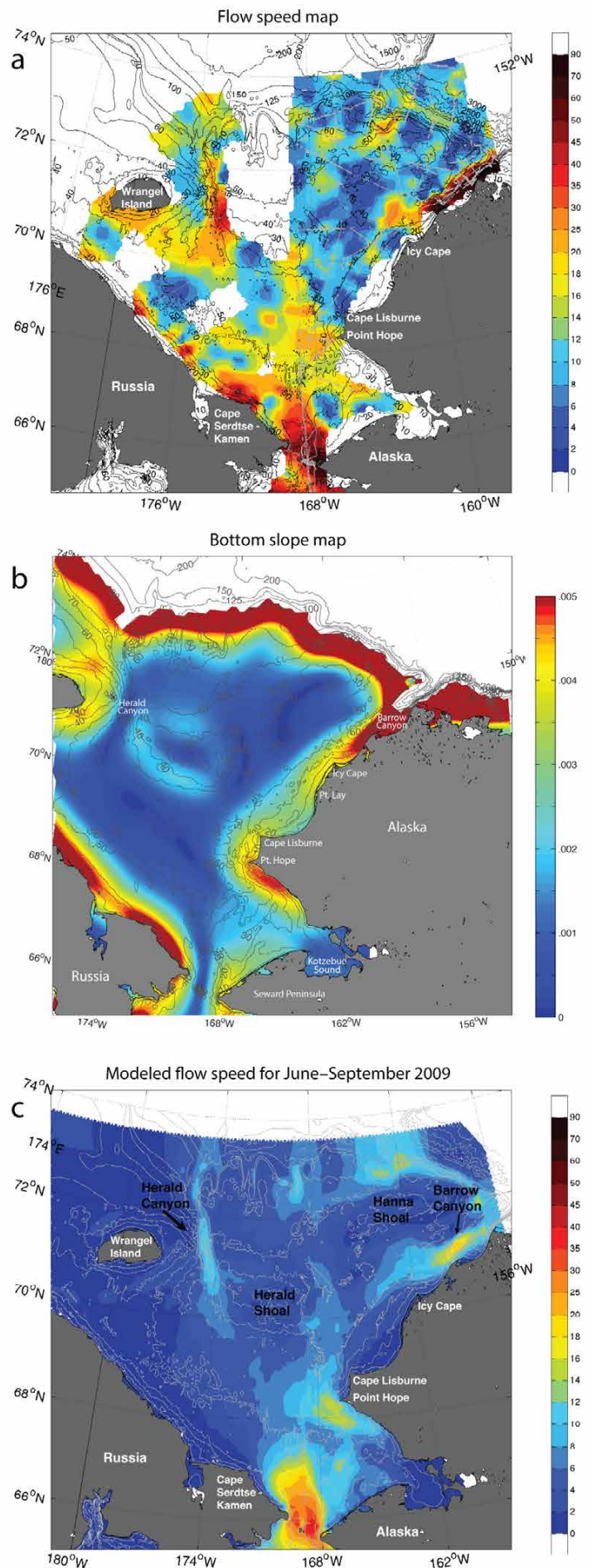
bryozoans, ascidians) need large volumes of water passing by for food supply; hence, they are more likely to thrive in a high-flow environment (von Dassow, 2005). On the other hand, deposit feeders (e.g., many polychaetes, some sea cucumbers, some bivalves as well as sipunculids) require high deposition rates of organic particles, which is more likely when the currents are weak (Wlodarska-Kowalczuk and Pearson, 2004; Wildish and Kristmanson, 2005; Grebmeier et al., 2006; Nelson et al., 2014). Here, we use maps of benthic biomass for both epifauna and macrofauna, where we distinguish the respective proportion of suspension feeders versus deposit feeders (Figure 3). Our goal is to evaluate how well feeding guild distributions within benthic communities align with our understanding of the flow speed patterns across the Chukchi shelf.

Epifaunal suspension feeders prevail in the region close to the Alaskan coast, particularly from Pt. Hope north to Barrow Canyon (Figure 3a), aligning well with the presence of the swift ACC. Even though the ACC slows between Cape Lisburne and Icy Cape in our flow speed map (Figure 2a), the bottom slope is still relatively large there (Figure 2b). Also, the ACC undoubtedly meanders to some degree, and we suspect that the integrating nature of the benthic fauna is likely more representative of the long-term

conditions than our flow map. There is also an enhanced percentage of suspension feeders on the eastern side of Herald Shoal near the entrance to the Central Channel, consistent with the flow speed map. The other two expected locations of enhanced suspension feeders are Bering Strait and the eastern side of Herald Canyon. However, while the combined suspension and deposit feeder epifaunal biomass is large in both regions, the limited benthic data available for these regions indicate variable faunal feeding types (Figure 3a). We note that the seafloor in Bering Strait is primarily composed of rock and gravel, making it challenging to impossible to trawl or take grabs. Hence, the few stations occupied on the eastern side of the strait are not representative (plus, our mapping may be biased as we don't include the predator component in the analysis).

The limited samples from the eastern side of Herald Canyon indicate that most fauna are deposit feeders (dominated by the sea star *Ctenodiscus crispatus*), whereas the western flank, with lower observed and modeled flow speeds, is dominated by suspension feeders. This pattern is opposite from what is expected and may be the result of variable canyon flow. As noted above, benthic fauna are indicative of long-term conditions, yet the flow speed map is composed of data

from only summer and fall. It may be that, averaged over the full year, the flow in the canyon is significantly different than that shown in Figure 2a. Alternatively, the epibenthos and the macrofauna may possibly be more versatile and opportunistic than previously thought, and in locations of high variability in flow and substrate, such as Herald Canyon, a wider diversity in feeding types may prevail. In general, epifaunal deposit feeder biomass is proportionally higher than that of suspension feeders on the north-central part of the shelf (Figure 3a), consistent with the generally weak velocities in this region.

The distribution of macrofauna shows similar characteristics to that of the epifauna (Figure 3b). In particular, there are high percentages of suspension feeding macrofauna along the path of the ACC into Barrow Canyon, as well as near the entrance of the Central Channel. As was true with the epifauna, macrofaunal biomass of suspension and deposit feeders is generally low on the north-central shelf. Furthermore, the pattern in Herald Canyon is similar to that of the epifauna (i.e., more deposit feeders on the eastern flank and more suspension feeders on the western flank), in contrast to what is expected based on the flow speed map. This observation further supports the notion that the summer-only flow measurements in Herald Canyon may not
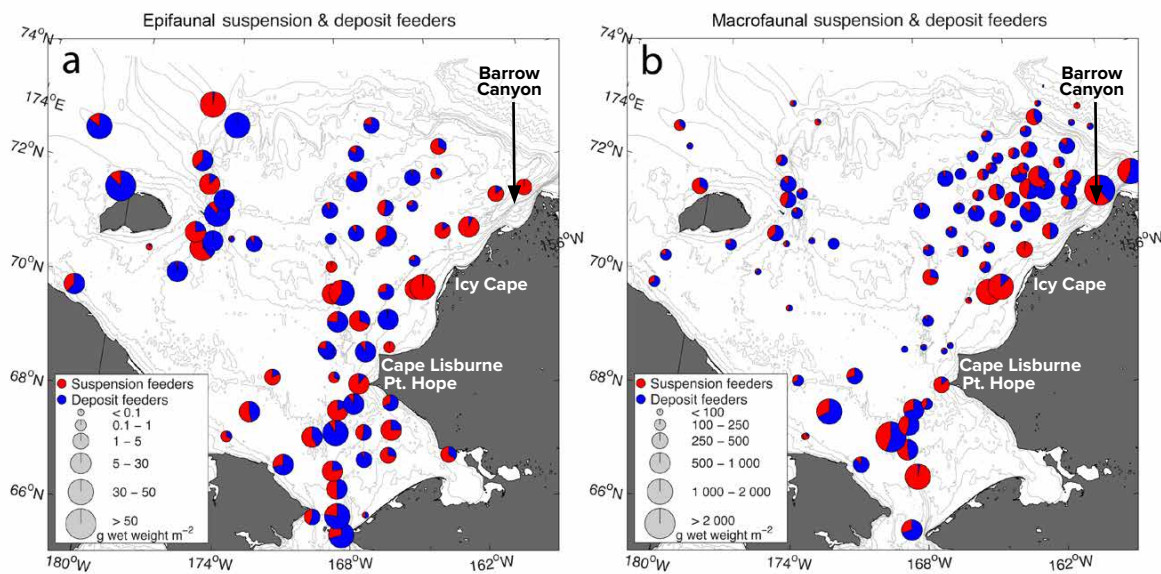

FIGURE 3. Ratio of epifaunal (a) and macrofaunal (b) suspension feeders (red) to deposit feeders (blue) for stations on the Chukchi shelf. The diameter of the pie charts is proportional to the total biomass (g wet weight m^{-2}) of the sample. The gray contours are the bottom depth.

be representative of the year-round flow speed conditions there. As was true for the epifauna, the limited ability to sample macrofauna in Bering Strait biases any interpretations there. However, the percentage of suspension feeders just north of the strait is high; this is likely because of the change to a softer bottom in this region (hence, more representative sampling), where the flow speeds are still quite strong.

Relation to Sediment Grain Size

Different species of benthic organisms prefer specific types of sediment composition and deposition (Grebmeier et al., 2006; Blanchard and Feder, 2014). We expect that finer sediments are washed out in the regions of relatively high flow and are deposited where the currents are slower. Overall, our map of modal grain size (Figure 4) supports this notion. The flow path of the ACC along the Alaska coast and strong flow into Barrow Canyon are both evident in deposits of coarser sediments. This is true as well for the high velocities in Bering Strait. In addition, there is evidence of the Central Channel pathway (although the small modal values on top of Hanna Shoal cannot be put into context with the flow field because there are no velocity data from there). There is even a signature of the enhanced flow on the southeastern side of Herald Shoal and just south of Wrangel Island, both of which are seen in Figure 2a. The grain sizes in Figure 4 also correlate well with the benthic feeding types, in particular, the suspension feeders found in the ACC, Barrow Canyon, and at the entrance to the Central Channel.

ATMOSPHERIC FORCING

Until now, we have considered the long-term patterns in the Chukchi Sea, that is, signals that are not associated with year-to-year changes or seasonal (or shorter time scale) variability. The flow speed maps excluded periods of strong winds and anomalous currents, and the benthic fauna and sediment characteristics are integrative by nature and hence are

not sensitive to short-term variability. We now undertake a comparative analysis of the three broad-scale RUSALCA biophysical surveys conducted in 2004, 2009, and 2012. These data provide the opportunity to address interannual changes in the hydrography of the shelf during the late summer to early autumn time period—and how these changes might in turn be related to measured biological signals in the water column. We begin with a description of the atmospheric forcing at work during the time periods of the three RUSALCA cruises.

In August 2004, when the RUSALCA survey took place, moderately strong southerly and southeasterly winds prevailed (Figure 5a) associated with a well-developed Beaufort High (anticyclonic circulation) north of Canada and an Aleutian Low (cyclonic circulation) in the southeastern Bering Sea. While the Beaufort High signal is not unexpected, such an Aleutian Low signature is anomalous for the month of August (Favorite et al., 1976). In contrast, during the RUSALCA surveys in September

2009 and 2012, the winds were out of the north/northeast across the Chukchi Sea (Figure 5b,c). While this is consistent with the seasonal shift in winds from late summer to early fall, there were anomalous aspects to September 2009 and 2012. As discussed in detail by Pisareva et al. (2015), in 2009 the Aleutian Low signature was shifted to the east and there was a strong Siberian High signature, both of which were conducive for the enhanced northerly winds over the Chukchi shelf. In 2012, the Siberian High was also present, contributing to the strong northerly winds in September (the Aleutian Low was in its normal position for that time of year).

Winds impact SSTs in the Chukchi Sea as well as the distribution of the pack ice in the region. As described by Wood et al. (2015, in this issue), the 2004 survey was conducted during the warmest period of the three RUSALCA years, which is reflected in the mean SST for that month (Figure 5d). Warm water was advected northward through Bering Strait and spread through much of the shelf, even reaching Herald Canyon. Sea
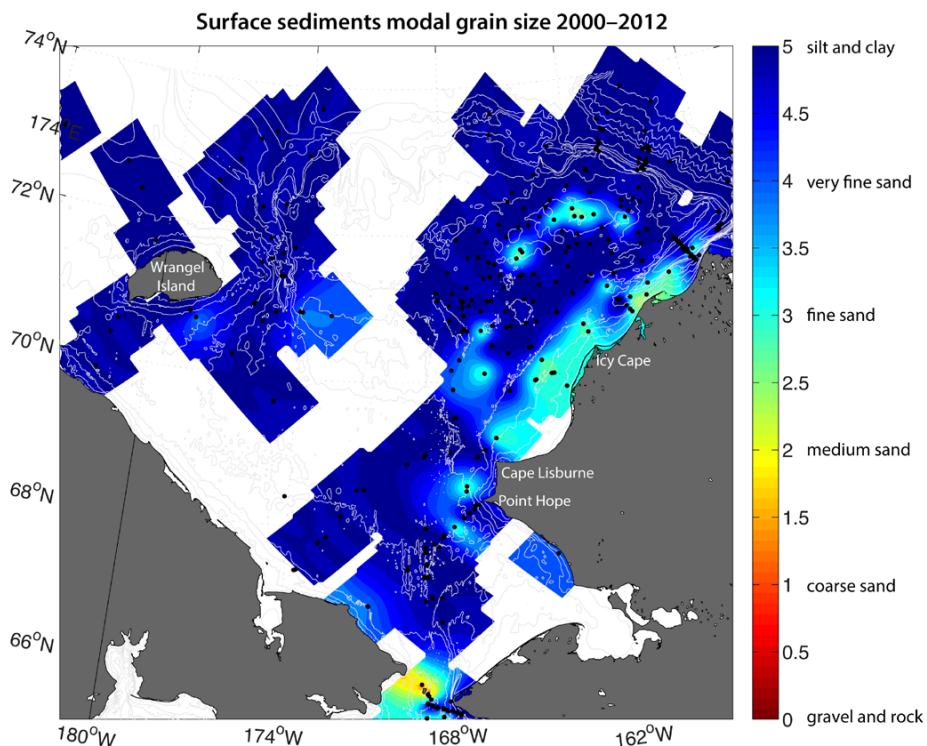

FIGURE 4. Map of prevailing surface sediment modal grain size for 2000 to 2012. See the legend for the modal size definitions. The gray contours are bottom depth.

ice was present only in the far western part of the Chukchi shelf into the East Siberian Sea (Figure 5d). In contrast, SSTs during the 2009 survey were significantly cooler, which is not surprising since the survey was conducted roughly a month later in the season than the 2004 survey (Figure 5e). Furthermore, there was almost no sea ice present in the region due to the enhanced easterly and southeasterly winds earlier in the summer, which tended to advect ice off of the shelf (Wood et al., 2015, in this issue). Despite the cooler SSTs in 2009, there was a tongue of warm water extending from Hope Valley to the northwest into Herald Canyon. This was associated with Alaskan Coastal Water, which was diverted to the west due to the aforementioned northerly winds during that month (Pisareva et al., 2015). The dominant SST signals in 2012 were a very warm band along the coast of Alaska signifying the ACC, and a cold band along the Russian continent associated with the

SCC (Figure 5f). Despite the record low sea ice extent in 2012 (e.g., Timmermans et al., 2012), large amounts of ice were present locally in the Chukchi Sea throughout the summer because of generally weak winds and cooler surface temperatures (Wood et al., 2015, in this issue).

INTERANNUAL HYDROGRAPHIC VARIABILITY OF THE CHUKCHI SEA
Water Mass Definitions
The water mass characteristics of the Chukchi Sea vary both on long and short time scales, due to a variety of factors. For instance, there are year-to-year changes in the properties of the water advected through Bering Strait from the Pacific, and, once in the Chukchi, processes such as wind mixing and ice formation/melt further alter the water. Thus, there are no permanent, precise temperature-salinity (T-S) boundaries between the different water masses; oftentimes these boundaries

are vague and they do not remain the same over time. Nonetheless, the core characteristics of the main water masses are straightforward to identify. Following the methodology of Pisareva et al. (2015), we identified three Pacific-origin water masses—Alaskan Coastal Water (ACW), Bering Summer Water (BSW), and Pacific Winter Water (WW)—which were present in the domain in all three surveys. The two Arctic-origin water masses—Atlantic Water (AW) and Siberian Coastal Water (SCW)—were observed more sporadically. In particular, AW was measured only in 2009 at the northernmost transect in Herald Canyon, while SCW was present in the SCC only during the latter two surveys.

Lateral Water Mass Distributions
We now construct lateral distributions of the four prevailing water masses (ACW, BSW, SCW, and WW) for each of the RUSALCA surveys. Then, in the section
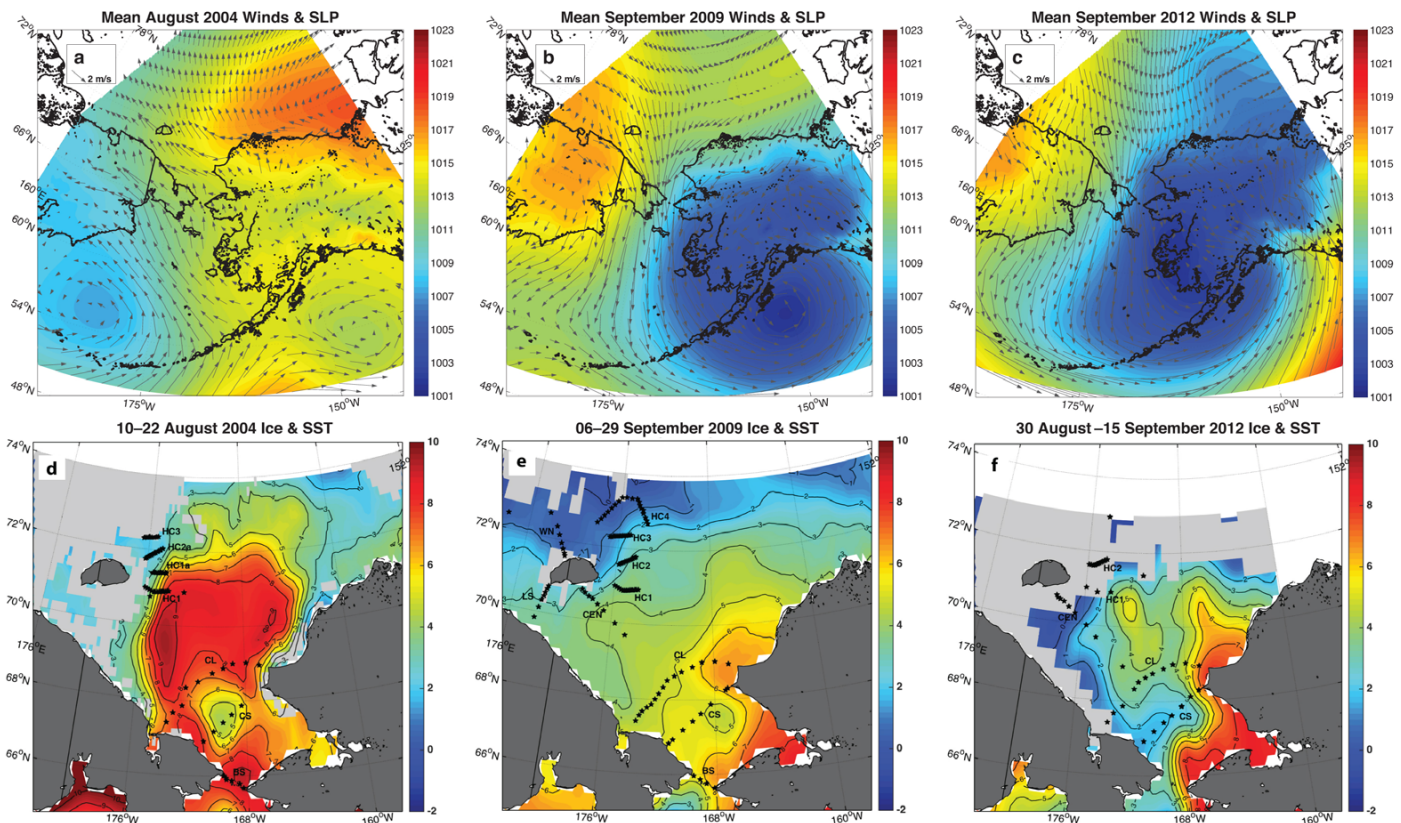

FIGURE 5. Mean sea level pressure (color, mb) and 10 m wind (vectors) for (a) August 2004, (b) September 2009, and (c) September 2012, using the North American Regional Reanalysis data. Mean sea surface temperature (°C, color) and ice cover (gray shading) for the periods of the RUSALCA surveys in (d) 2004, (e) 2009, and (f) 2012, using AVHRR–AMSRE data.

on Lateral Zooplankton Distributions, we relate these water masses to the distribution of the different zooplankton groups observed during the cruises.

2004 RUSALCA Survey

In 2004, both ACW and BSW were advecting northward through Bering Strait (Figure 6a,b); the ACW was confined to the eastern side of the strait while the BSW was present on the western side, which is the typical configuration during the summer months. Unfortunately, the Chukchi South (CS) transect had no CTD stations close to the Alaskan coast, but we assume that ACW was present there because of the zooplankton data (see Lateral Zooplankton Distributions section), plus ACW was present just to the north adjacent to Cape Lisburne. This is consistent with the known pathway of the ACC, which advects ACW northeastward toward Barrow Canyon (Coachman et al., 1975). Notably, ACW was distributed broadly across the Chukchi shelf along the Cape Lisburne (CL) line (in the upper part of the water column) all the way to the Chukotka coast. This water mass can also be seen on the SST map for the period of the 2004 survey (Figure 5d). There is even evidence of ACW on the eastern side of Herald Canyon on transects HC1 and HC1a.

As noted earlier, 2004 was the warmest of the RUSALCA years, so an alternative explanation for the warm water on the western side of the CL line and in Herald Canyon is that it was heated locally on the shelf, rather than emanating from the ACC (e.g., transformed BSW or meltwater). This explanation is more consistent with the winds during this period, which were predominantly from the southeast and relatively stable (Figure 5a). Such winds would not tend to divert the ACW from the coast. As discussed in Pisareva et al. (2015), strong northerly winds can lead to a transposition of the ACW and the BSW in Bering Strait whereby the ACW spreads to the western shelf and into Herald Canyon. Pisareva et al. (2015) demonstrate that

when the time integral of the wind stress during a northerly wind event exceeds a certain threshold, this leads to such conditions. Using the data from Pisareva et al. (2015; their Figure 16), we find that only one northerly wind event barely reached the threshold, and this occurred after the RUSALCA survey. Hence, we have no dynamical explanation for the presence of ACW on the western shelf and in Herald Canyon during August 2004. Nonetheless, this water falls into the temperature, salinity, and silicate range of ACW, and this interpretation is supported by the zooplankton data (see below).

The lateral distribution of BSW on the Chukchi shelf in August 2004 (Figure 6b) is consistent with previous studies (e.g., Coachman et al., 1975). North of Bering Strait, BSW progresses through Hope Valley and continues into Herald Canyon, confined to the eastern flank. WW was only measured in Herald Canyon in 2004 (Figure 6c). As discussed in detail in Pickart et al. (2010), a large portion of this water mass entered the canyon on the western flank and, as it progressed northward, switched to the eastern side of the canyon.

2009 RUSALCA Survey

Pisareva et al. (2015) discuss the lateral water mass distributions for the 2009 survey in detail. Here, we reproduce their maps for completeness and also because in the Lateral Zooplankton Distributions section, we compare these distributions to the zooplankton measurements. As noted above, September 2009 was characterized by strong northerly winds, which diverted the ACW onto the western Chukchi shelf and into Herald Canyon (Figure 7a). In general, the distributions of BSW and WW in 2009 (Figure 7b,d) were similar to those in 2004 (Figure 6b,c). Other than Bering Strait (where in 2009 the BSW was found on the eastern side of the strait compared to the western side in 2004), distribution of BSW was quite similar in both surveys. WW was again only present in the very northwest part of the shelf (during the

2009 survey, sections occupied all around Wrangel Island revealed the presence of this water), although the WW in 2004 had been more recently ventilated (see Pickart et al., 2010, and Johanna Linders, University of Gothenburg, *pers. comm.*,
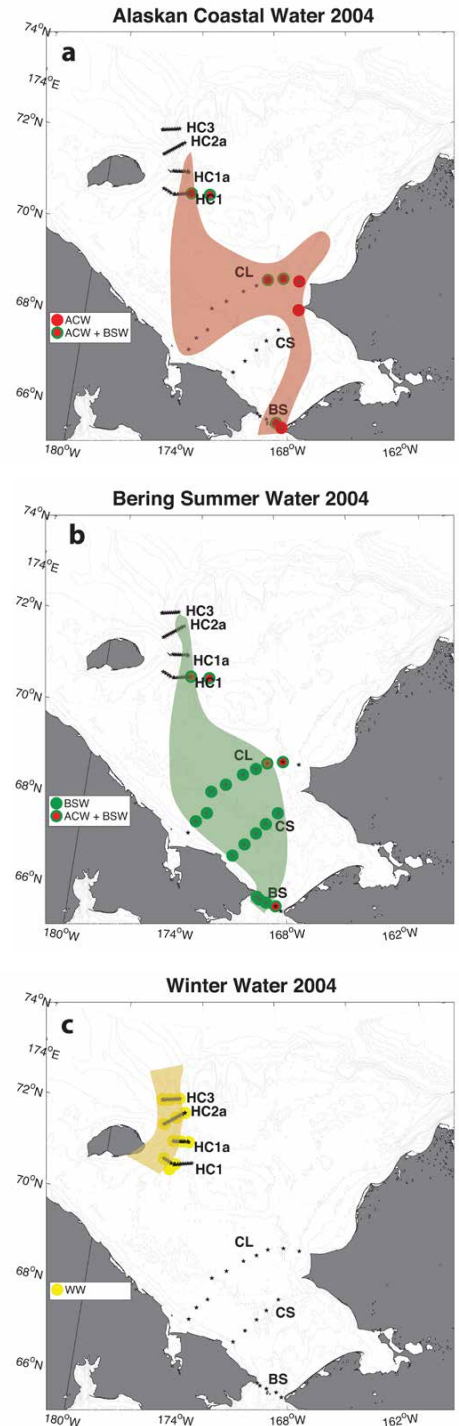

FIGURE 6. Lateral distributions of water masses for the 2004 RUSALCA survey. The colored circles indicate the zooplankton clusters for each of water mass, identified in samples collected during the survey.

2015). The biggest difference between the 2004 and 2009 surveys was the presence of SCW in 2009 (Figure 7c). As discussed in Pisareva et al. (2015), the SCC was advecting this water mass southeastward along the Chukotka coast toward Bering Strait. Furthermore, SCW was flowing anticyclonically around Wrangel Island.

2012 RUSALCA Survey

Unfortunately, the Bering Strait (BS) section (see Figure 7 for location) was not sampled in 2012 due to harsh weather conditions, and the coverage in Herald Canyon was far less than in the previous two cruises. Nonetheless, there was sufficient coverage to make lateral maps for this survey. The ACW was confined to the coastal pathway (Figure 8a), which could be considered surprising based on the strong northerly winds in September

2012. The average wind speed in the vicinity of Bering Strait that month was greater than in September 2009 (Figure 5), yet in 2009 wind forcing caused the ACW to be transported to the northwest part of the shelf (Pisareva et al., 2015). However, the wind was steadier in 2012 than in 2009, and was the reason for the larger monthly mean wind speed. When considering the wind time series in Bering Strait, there were no wind events in 2012 in which the time integral of the wind stress exceeded the threshold for water mass transposition in the strait, as was true for the 2009 event analyzed in Pisareva et al. (2015).

The distribution of BSW in 2012 was similar to that of the other two RUSALCA surveys (although BSW was closer to the Alaskan Coast in 2012; Figure 8b). As was true in 2009, the SCC was present in 2012, and consequently SCW was measured

from southeast of Wrangel Island toward Bering Strait along the Russian coast (Figure 8c). The fact that SCW was measured along the Central Chukchi (CEN) section suggests that the water was likely circulating around Wrangel Island, as was the case in 2009. The unexpected aspect of the 2012 survey was the WW distribution. In addition to being observed in Herald Canyon, the Winter Water was measured adjacent to the Chukotka coast in the CL and CS transects (Figure 8d). To our knowledge, this is the first time that WW has been detected in this region during summer.

We now relate these observed lateral patterns of water masses in the different RUSALCA surveys to the measured distributions of zooplankton communities.

Lateral Zooplankton Distributions

Overall, the lateral distributions of zooplankton communities correspond very well with the water mass patterns described above. In Figures 6 to 8, we identify the zooplankton clusters associated with each of the water masses in question. We note that the vertical net tows provide an integrated measurement through the water column, and therefore multiple zooplankton communities were sometimes present at a given station (e.g., Ershova et al., 2015). Those instances are identified in the figures. The reader should also note that net tows were not carried out at all of the sites. We now examine the general zooplankton patterns in each of the surveys and remark on several notable samples.

2004 RUSALCA Zooplankton Communities

In 2004, Alaskan coastal zooplankton communities were found close to the coast of Alaska on the three southern transects (BS, CS, and CL, Figure 6a), consistent with the known pathway of the ACC. As discussed above, ACW was present across the entire length of the CL transect, according to the T-S characteristics measured by the CTD. However, this water mass was identified only in the upper
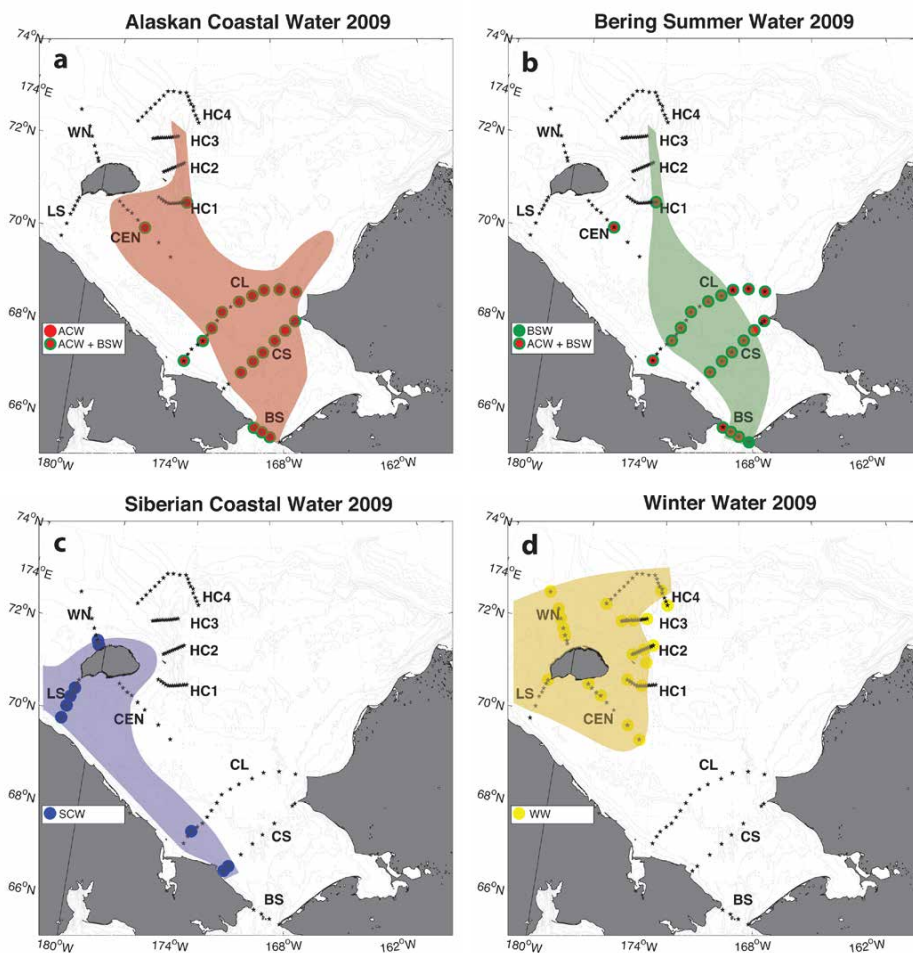

FIGURE 7. Lateral distributions of water masses for the 2009 RUSALCA survey. The colored circles indicate the zooplankton clusters for each of water mass, identified in samples collected during the survey.

layer, and, consequently, the integrated zooplankton samples outside of the ACC were dominated by Bering Sea Water species (Figure 6b). Nonetheless, all of these stations contained coastal neritic species such as cladocerans *Evadne nordmanni* and *Podon leuckarti* and copepods *Eurytemora* spp., *Acartia hudsonica*, and *Tortanus discaudata*, as well as a variety of meroplankton. Our observation in the 2004 RUSALCA Survey section above that ACW was present in Herald Canyon during this survey is also supported by the zooplankton data, as a significant presence of Alaskan coastal zooplankton were found at the head of the canyon (and to the east of the canyon).

Zooplankton species characteristic of Bering Sea Water (e.g., *Metridia pacifica, Eucalanus bungii, Neocalanus* spp.) were dominant over most of the southern shelf, extending into Herald Canyon, consistent with the water mass pattern (Figure 6b). Notably, the station closest to Koluchinskaya Bay along the Chukotka coast (near 174°W) contained the lowest biomass of zooplankton of all of the stations in the survey. The CTD data at that site showed that, although ACW was present in the top layer, closer to the bottom the water was slightly saltier, significantly colder (< –1.4°C), and elevated in silicate. This is outside of the temperature range of BSW but fresher than WW. Therefore, we suspect that this water emanated from Koluchinskaya Bay. As seen in Figure 6c, the WW communities of zooplankton coincide quite well with the presence of WW throughout much of Herald Canyon.

2009 RUSALCA Zooplankton Communities

The Alaskan coastal species and Bering Sea species were co-located on many more stations in 2009 compared to 2004 (Figure 7a,b). In some respects, this observation is in line with the hydrographic characteristics measured in the two surveys. For example, the ACW in the central Chukchi shelf and in Herald Canyon occupied more of the water column in 2009, which explains why the

Bering Sea species did not dominate at these stations. Perhaps surprisingly, the stations adjacent to the Alaskan coast on the CS and CL transects contained Bering Sea clusters but no obvious evidence of BSW. One should keep in mind, however, that the northerly winds in September 2009 caused a transposition of the ACW and BSW in Bering Strait (indeed, note the dominant presence of the Bering Sea zooplankton cluster on the eastern side of Bering Strait). This likely resulted in BSW progressing northward along the Alaskan Coast prior to our survey, perhaps mixing with the ACW during the relaxation phase of the event.

As discussed above in the 2009 RUSALCA Survey section, SCW was being advected in 2009 toward Bering Strait along the Chukotka coast in the SCC, and it was also identified around Wrangel Island presumably being transported by the anticyclonic circulation around the island (Pickart et al., 2010). This is in good agreement with the zooplankton data, which show Siberian species both along the Siberian coast and on the Wrangel North (WN) transect (Figure 7c). This latter observation is significant, as it verifies the unexpected presence of SCW north of Wrangel Island. As was the case in 2004, the station closest to Koluchinskaya Bay along Chukotka coast was anomalous. Despite the fact that SCW occupied the entire water column at that site, the zooplankton data revealed the presence of communities from both Alaskan coastal waters and the Bering Sea (Figure 7a,b). This could be due to both types of zooplankton species entering the bay during earlier periods (the Bering species carried by BSW during moderate
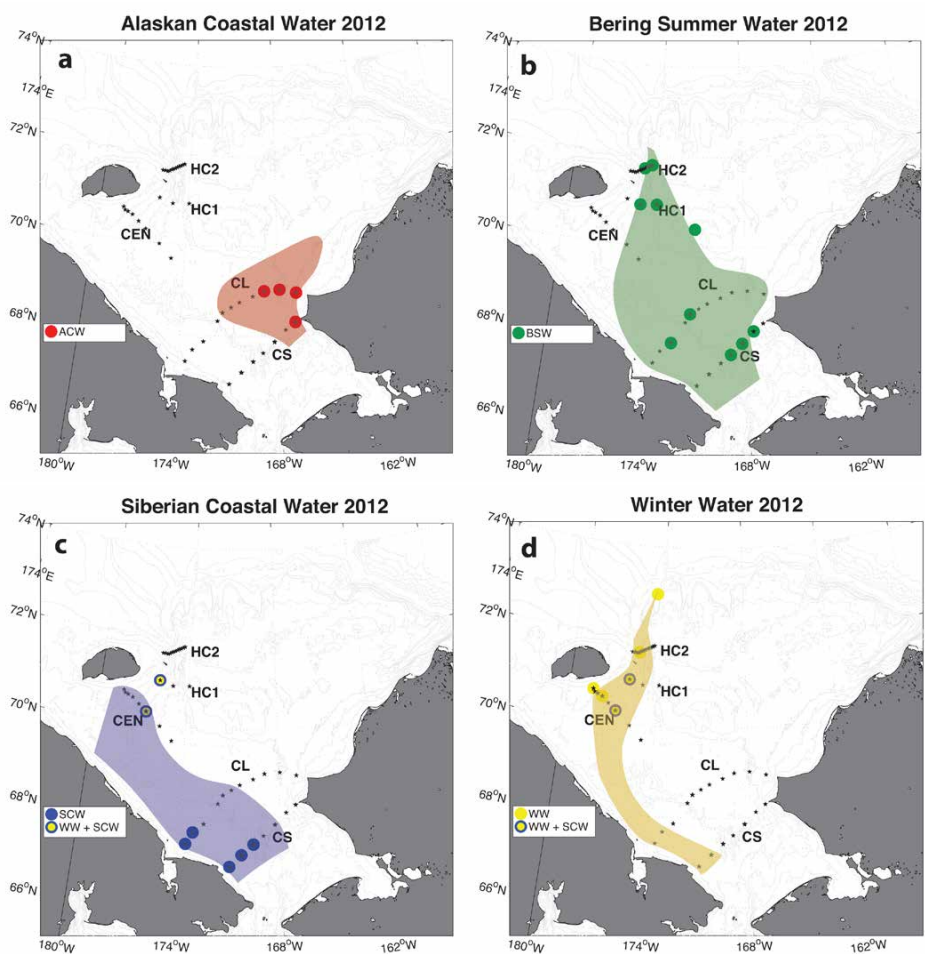

FIGURE 8. Lateral distributions of water masses for the 20012 RUSALCA survey. The colored circles indicate the zooplankton clusters for each of water mass, identified in samples collected during the survey.

wind conditions, and the Alaskan species advected with ACW during the strong northerly wind event) and subsequently flushing out of the bay and mixing with the SCW. Finally, as was true for 2004, the WW measured in 2009 contained predominantly Winter Water zooplankton species (Figure 7d).

2012 RUSALCA Zooplankton Communities

For the 2004 and 2009 data sets, using species abundance versus biomass matrices produced very similar results (although they emphasize a different set of taxa). However, in 2012, analyzing these two matrices produced slightly different results—in particular, for the region near the Siberian coast (see below). Hence, for 2012 we show the cluster analysis results based on biomass as they are in better overall agreement

with the hydrographic data. As shown above, the ACW in 2012 was confined to the region near the Alaskan coast, and this is borne out as well by the distribution of the Alaskan zooplankton clusters (Figure 8a). Good agreement also exists between the BSW and Bering Sea clusters (Figure 8b), including evidence that this water mass carries the Bering Sea species into Herald Canyon.

As was the case in 2009, SCW was present in 2012 adjacent to the Siberian coast and near Wrangel Island in accordance with the Siberian zooplankton clusters (Figure 8c, although the net tow sample along the CEN line southeast of Wrangel Island also showed evidence of WW species). Recall that the most notable aspect of the 2012 survey was the presence of WW along the Chukotka coast (Figure 8d). The cluster analysis of community biomass for 2012

shows no evidence of this; the reason is that the hydrozoan jellyfish *Halitholis cirratus,* which is more characteristic of Siberian coastal communities, dominates the biomass for stations along the southwest ends of the CL and CS transects. However, the stations in question also contain a number of WW species, including several ice-associated organisms, such as the amphipod *Apherusa glacialis* and the copepod *Jaschnovia brevis*. These species constitute a very small percentage of community biomass and therefore do not influence the separation of clusters. This supports our interpretation based on the hydrography that WW was present this far to the south in September 2012.

Vertical Plankton Distributions

Finally, we consider some aspects of the distribution of plankton (copepods, diatom chains) vertically in the water column described using the AVPR data, and assess the patterns in relation to the hydrographic structure on the shelf. In addition to the physical variables, we include chlorophyll fluorescence (herein fluorescence; measured by the CTD) and silicate (analyzed from the water samples). We focus on two transects occupied during the RUSALCA 2009 survey—the CL line (i.e., the central shelf) and the HC3 line (Figures 9 and 10).

As discussed above, three water masses were present on the CL section in 2009 (Figure 9): moderately warm and very fresh SCW proceeding southwestward and confined to the coastal region of Chukotka; seaward of this, very warm and moderately fresh ACW occupying most of the section up to the Alaska Coast; and a lens of relatively cold, salty BSW situated near the bottom in the central portion of the transect, characterized by elevated silicate. Both the ACW and BSW were being advected to the northwest. As Pisareva et al. (2015) show, the ACW advected all the way into Herald Canyon by wind forcing, and on section HC3 it occupied the upper layer on the eastern side of the canyon (with a small, isolated
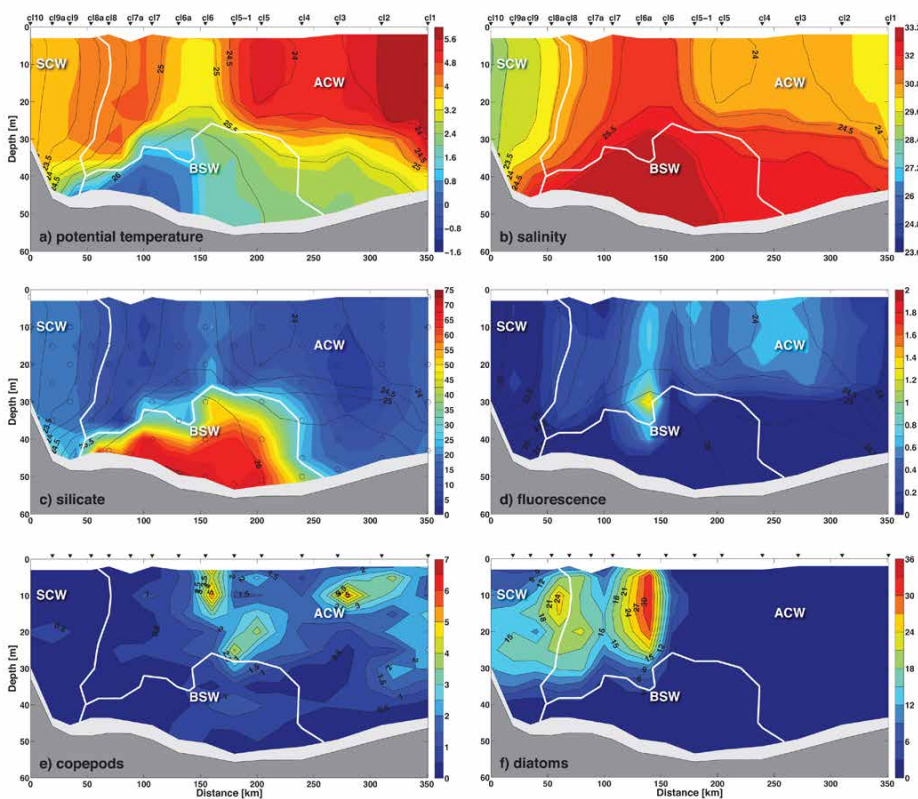

FIGURE 9. Vertical sections of (a) potential temperature (°C), (b) salinity, (c) silicate (μmol L^{-1}; circles denote water sample locations), (d) fluorescence (mg mL^{-1}), (e) copepods (# L^{-1}), and (f) diatoms (# L^{-1}) for the Cape Lisburne (CL) line occupied during the September 2009 RUSALCA cruise. The view is to the northwest. The black contours are potential density (kg m^{-3}). The approximate boundaries between water masses (marked with labels) are represented by thick white lines. The black inverted triangles mark the station positions, with the station names above them.

lens of ACW located in the center of the canyon, Figure 10). The deep layer in the canyon was predominantly WW, which is also high in silicate. The final water mass in the canyon was meltwater, due to the melting of sea ice on the western flank.

Copepods were prevalent within the ACW on the CL line (Figure 9e), advected with the water as it progressed northward through Bering Strait. Notably, there was little to no correspondence between the copepods and diatom chains (compare Figure 9e,f); the latter were abundant in the SCW and highly concentrated at the lateral boundary between the SCW and ACW (Figure 9f). This could be due to frontal dynamics that helped trap phytoplankton between the southward-flowing SCC and the northward flow of ACW (investigation of such dynamics is beyond the scope of this study). There was little correspondence between fluorescence and diatom chain distribution, suggesting that the fluorescence signal in the ACW was due to smaller phytoplankton prey that likely supported the copepods within the ACW (Figure 9d). However, the largest fluorescent signal was associated with the large concentration of diatom chains in the frontal region where they could be utilized by the copepods. The low fluorescence signal and high diatom chain abundance in the western SCW, extending to depth, suggest that the diatom chains in that water mass were senescent, not fluorescing, and sinking.

By the latitude of Herald Canyon, the copepods were deeper in the water column, the majority of them situated at the base of the pycnocline (at the interface between the ACW and WW, Figure 10e). Fluorescence was elevated at this level of the water column (Figure 10d), indicating healthy phytoplankton that were being sustained on the elevated nutrients found below the pycnocline and that provided prey for the co-located copepods. However, as was true farther south, it is likely that the copepods were feeding on smaller phytoplankton in addition to diatoms. To wit, the strongest diatom signal was to the west of the main core of

ACW in the small isolated lens of this water that had a negligible number of copepods. The other region with a large diatom chain population was within the core of ACW on the eastern end of the section, and it also had no trace of copepods. Rather, the copepods at these eastern locations were deeper in the water column, in association with the pycnocline where alternative prey could be concentrated. (It is unclear at this point why diatoms were absent from the ACW in the central shelf but present in this water mass in Herald Canyon.)

It is important to note that, in summer in the Chukchi Sea, copepods may graze preferentially on microzooplankton (Campbell et al., 2009), prey that are not described using the AVPR. The fact that copepods were present within (or at the base of) the ACW in both the CL and HC3 sections indicates that there are biological

implications to the wind-driven transposition of water masses in Bering Strait; namely, that Pacific-origin zooplankton within the coastal water can be advected to the northwest part of the Chukchi Sea and presumably fluxed into the basin as the water exits Herald Canyon.

CONCLUSIONS

In this study, we used data from three biophysical cruises—August 2004, September 2009, and September 2012—that sampled both the US and the Russian sectors of the Chukchi Sea as part of the RUSALCA program. These data were supplemented with information from various other programs carried out in US waters. A depth-averaged flow speed map was constructed for the shelf that showed stronger currents within the lateral constrictions of Bering Strait, Barrow Canyon, and Herald Canyon. In addition,
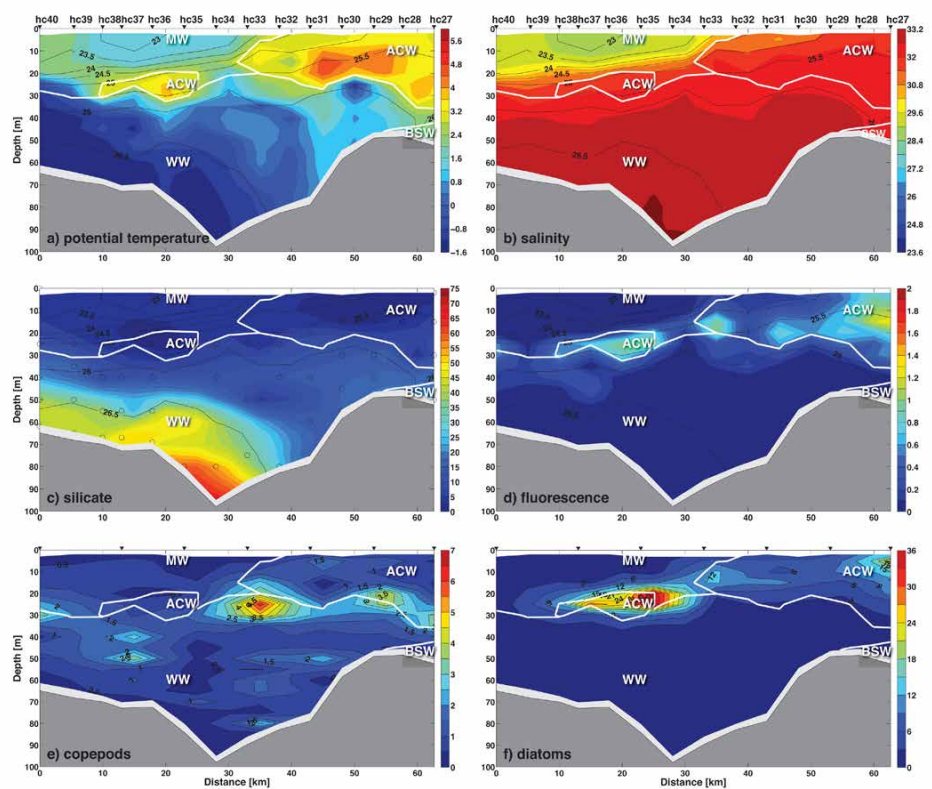

FIGURE 10. Vertical sections of (a) potential temperature (°C), (b) salinity, (c) silicate (µmol L^{-1}; circles denote water sample locations), (d) fluorescence (mg mL^{-1}), (e) copepods (# L^{-1}), and (f) diatoms (# L^{-1}) for the Herald Canyon (HC3) line occupied during the September 2009 RUSALCA cruise. The view is to the northwest. The black contours are potential density (kg m^{-3}). The approximate boundaries between water masses (marked with labels) are represented by thick white lines. The black inverted triangles mark the station positions, with the station names above them.

flow speeds were enhanced adjacent to the Alaska coast (the Alaskan Coastal Current) and Russian coast (the Siberian Coastal Current). The local bottom slope dictated variations within the Alaskan Coastal Current. The observed flow speed patterns were consistent with output from a numerical model. It was demonstrated that, for the most part, epifaunal and macrofaunal suspension feeders were found in greater abundance in regions of stronger flow, while deposit feeders were dominant in areas where the currents were weaker (the major exception being in Herald Canyon). The patterns of zooplankton on the shelf were different for each of the RUSALCA cruises. This was shown to be dictated predominantly by the distribution of Pacific and Siberian water masses at the times of the surveys. Our results highlight relationships between the physical environment and the biology of the Chukchi shelf on time scales of many years to decades for the benthos, and weeks to months for the water column. ⌾

REFERENCES

Appeltans, W.P., P. Bouchet, G.A. Boxshall, C. De Broyer, N.J. de Voogd, D.P. Gordon, B.W. Hoeksema, T. Horton, M. Kennedy, J. Mees, and others. 2012. World register of marine species, http://www.marinespecies.org.

Ashjian, C.J., S.M. Gallager, and S. Plourde. 2005. Transport of plankton and particles between the Chukchi and Beaufort Seas during summer 2002, described using a Video Plankton Recorder. *Deep Sea Research Part II* 52:3,259–3,280, http://dx.doi.org/10.1016/j.dsr2.2005.10.012.

Blanchard, A.L., and H.M. Feder. 2014. Interactions of habitat complexity and environmental characteristics with macrobenthic community structure at multiple spatial and temporal scales in the northeastern Chukchi Sea. *Deep Sea Research Part II* 102:132–143, http://dx.doi.org/10.1016/j.dsr2.2013.09.022.

Blanchard A.L., C.L. Parris, A.L. Knowlton, and N.R. Wade. 2013. Benthic ecology of the northeastern Chukchi Sea: Part II. Spatial variation of Megafaunal Community Structure, 2009–2010. *Continental Shelf Research* 67:67–76, http://dx.doi.org/10.1016/j.csr.2013.04.031.

Bluhm, B.A., K. Iken, S.L. Mincks, B.I. Sirenko, and B.A. Holladay. 2009. Community structure of epibenthic megafauna in the Chukchi Sea. *Aquatic Biology* 7:269–293, http://dx.doi.org/10.3354/ab00198.

Blumberg, A.F., and G.L. Mellor. 1987. A description of 3-D coastal ocean circulation model. Pp. 1–16 in *Coastal and Estuarine Sciences 4: 3-D Coastal Ocean Models*. N.S. Heaps, ed., American Geophysical Union, Washington, DC.

Brugler, E.T., R.S. Pickart, G.W.K. Moore, S. Roberts, T.J. Weingartner, and H. Statscewich. 2014. Seasonal to interannual variability of the Pacific Water Boundary Current in the Beaufort Sea. *Progress in Oceanography* 127:1–20, http://dx.doi.org/10.1016/j.pocean.2014.05.002.

Campbell, R.G., E.B. Sherr, C.J. Ashjian, S. Plourde, B.F. Sherr, V. Hill, and D.A. Stockwell. 2009. Mesozooplankton prey preference and grazing impact in the western Arctic Ocean. *Deep Sea Research Part II* 56:1,274–1,289, http://dx.doi.org/10.1016/j.dsr2.2008.10.027.

Cavalieri, D.J., J.P. Crawford, M.R. Drinkwater, D.T. Eppler, L.D. Farmer, R.R. Jentz, and C.C. Wackerman. 1991. Aircraft active and passive microwave validation of sea ice concentration from the Defense Meteorological Satellite Program Special Sensor Microwave Imager. *Journal of Geophysical Research* 96(C12):21,989–22,008, http://dx.doi.org/10.1029/91JC02335.

Coachman, L.K., K. Aagaard, and R.B. Tripp. 1975. *Bering Strait: The Regional Physical Oceanography*. University of Washington Press, Seattle and London, 172 pp.

Cooper, L.W., I.L. Larsen, T.M. Beasley, S.S. Dolvin, J.M. Grebmeier, J.M. Kelley, M. Scott, and A. Johnson-Pyrtle. 1998. The distribution of radiocesium and plutonium in sea ice-entrained Arctic sediments in relation to potential sources and sinks. *Journal of Environmental Radioactivity* 39(3):279–303, http://dx.doi.org/10.1016/S0265-931X(97)00058-1.

Cooper, L.W., A.S. Savvichev, and J.M. Grebmeier. 2015. Abundance and production rates of heterotrophic bacterioplankton in the context of sediment and water column processes in the Chukchi Sea. *Oceanography* 28(3):84–99, http://dx.doi.org/10.5670/oceanog.2015.59.

Davis, C.S., S.M. Gallager, M. Marra, and W.K. Stewart. 1996. Rapid visualization of plankton abundance and taxonomic composition using the Video Plankton Recorder. *Deep Sea Research Part II* 43:1,947–1,970, http://dx.doi.org/10.1016/S0967-0645(96)00051-3.

Davis, C.S., Q. Hu, S.M. Gallager, X. Tang, and C.J. Ashjian. 2004. Real-time observation of taxa-specific plankton distributions: An optical sampling method. *Marine Ecology Progress Series* 284:66–75, http://dx.doi.org/10.3354/meps284077.

Denisenko, S.G., J.M. Grebmeier, and L.W. Cooper. 2015. Assessing bioresources and standing stock of zoobenthos (key species, high taxa, trophic groups) in the Chukchi Sea. *Oceanography* 28(3):146–157, http://dx.doi.org/10.5670/oceanog.2015.63.

Dunton, K. 2015. Hanna Shoal: An integrative study of a High Arctic marine ecosystem. *ECO* 3(4):25–33, http://digital.ecomagazine.com/display_article.php?id=1986513&id_issue=254898.

Ershova, E.A., R.R. Hopcroft, and K.N. Kosobokova. 2015. Inter-annual variability of summer mesozooplankton communities of the western Chukchi Sea: 2004–2012. *Polar Biology* 38(9):1,461–1,481, http://dx.doi.org/10.1007/s00300-015-1709-9.

Feder, H.M., S.C. Jewett, and A.L. Blanchard. 2007. Southeastern Chukchi Sea (Alaska) macrobenthos. *Polar Biology* 30:261–275, http://dx.doi.org/10.1007/s00300-006-0180-z.

Feder, H.M., A.S. Naidu, S.C. Jewett, J.M. Hameedi, W.R. Johnson, and T.E. Whitledge. 1994. The northeastern Chukchi Sea: Benthos-environmental interactions. *Marine Ecology Progress Series* 111:171–190.

Grebmeier, J.M. 2012. Shifting patterns of life in the Pacific Arctic and sub-Arctic Seas. *Annual Review of Marine Science* 4:63–78, http://dx.doi.org/10.1146/annurev-marine-120710-100926.

Grebmeier, J.M., B.A. Bluhm, L.W. Cooper, S.L. Danielson, K.R. Arrigo, A.L. Blanchard, J.T. Clarke, R.H. Day, K.E. Frey, R.R. Gradinger, and others. 2015a. Ecosystem characteristics and processes facilitating persistent macrobenthic biomass hotspots and associated benthivory in the Pacific Arctic. *Progress in Oceanography* 136:92–114, http://dx.doi.org/10.1016/j.pocean.2015.05.006.

Grebmeier, J.M., B.A. Bluhm, L.W. Cooper, S.G. Denisenko, K. Iken, M. Kędra, and C. Serratos. 2015. Time-series benthic community composition and biomass and associated environmental characteristics in the Chukchi Sea during the RUSALCA 2004–2012 Program. *Oceanography* 28(3):116–133, http://dx.doi.org/10.5670/oceanog.2015.61.

Grebmeier, J.M., and L. Cooper. 2014. PacMARS Surface Sediment Parameters, Version 1.0., http://dx.doi.org/10.5065/D6416V3G.

Grebmeier, J.M., L.W. Cooper, H.M. Feder, B.I. Sirenko. 2006. Ecosystem dynamics of the Pacific-influenced Northern Bering and Chukchi Seas in the Amerasian Arctic. *Progress in Oceanography* 71:331–361, http://dx.doi.org/10.1016/j.pocean.2006.10.001.

Grebmeier, J.M., S.E. Moore, J.E. Overland, K.E. Frey, and R. Gradinger. 2010. Biological response to recent Pacific Arctic sea ice retreats. *Eos, Transactions American Geophysical Union* 91(18):161–162, http://dx.doi.org/10.1029/2010EO180001.

Favorite, F., A.J. Dodimead, and K. Nasu. 1976. Oceanography of the subarctic Pacific region, 1962–72. *Bulletin of the International North Pacific Fisheries Commission* 33:1–187.

Hibler, W.D. III. 1979. A dynamic and thermodynamic sea ice model. *Journal of Physical Oceanography* 9:15,959–15,969, http://dx.doi.org/10.1175/1520-0485(1979)009<0815:ADTSIM>2.0.CO;2.

Hu, Q., and C.S. Davis. 2005. Automatic plankton image recognition with co-occurrence matricies and support vector machine. *Marine Ecology Progress Series* 295:21–31, http://dx.doi.org/10.3354/meps295021.

Itoh, M., R.S. Pickart, T. Kikuchi, Y. Fukamachi, K.I. Ohshima, D. Simizu, K.R. Arrigo, S. Vagle, J. He, C. Ashjian, and others. 2015. Water properties, heat and volume fluxes of Pacific water in Barrow Canyon during summer 2010. *Deep Sea Research Part I* 102:43–54, http://dx.doi.org/10.1016/j.dsr.2015.04.004.

Lowry, K.E., R.S. Pickart, M.M. Mills, Z.W. Brown, G.L. Dijken, N.R. Bates, and K.R. Arrigo. 2015. The influence of winter water on phytoplankton blooms in the Chukchi Sea. *Deep Sea Research Part II* 118:53–72, http://dx.doi.org/10.1016/j.dsr2.2015.06.006.

MacDonald, I.R., B.A. Bluhm, K. Iken, S. Gagaev, and S. Strong. 2010. Benthic macrofaunal and megafaunal assemblages in the Arctic deep-sea Canada Basin. *Deep Sea Research Part II* 57:136–152, http://dx.doi.org/10.1016/j.dsr2.2009.08.012.

Mellor, G.L. 2004. *Users Guide for a 3-D, Primitive Equation, Numerical Ocean Model*. Atmospheric and Oceanic Sciences Program, Princeton University, 56 pp.

Mesinger, F., G. DiMego, E. Kalnay, K. Mitchell, P.C. Shafran, W. Ebisuzaki, D. Jović, J. Woollen, E. Rogers, E.H. Berbery, and others. 2006. North American regional reanalysis. *Bulletin of the American Meteorological Society* 87(3):343–360, http://dx.doi.org/10.1175/BAMS-87-3-343.

Münchow, A., and E.C. Carmack. 1997. Synoptic flow and density observations near an Arctic shelf break. *Journal of Physical Oceanography* 27:1,402–1,419, http://dx.doi.org/10.1175/1520-0485(1997)027<1402:SFADON>2.0.CO;2.

Nelson, J., R. Gradinger, B. Bluhm, J.M. Grebmeier, B. Sirenko, K. Conlan, P. Ramlal, S. Lee, H. Joo, B. Li, and others. 2014. Lower trophics: Northern Bering, Chukchi, Beaufort (Canada and US) Seas, and the Canada Basin. Pp. 269–336 in *The Pacific Arctic Region: Ecosystem Status and Trends in a Rapidly Changing Environment*. J.M. Grebmeier and W. Maslowski, eds, Springer, Dordrecht.

Paquette, R.G., and R.H. Bourke. 1974. Observations on the coastal current of Arctic Alaska. *Journal of Marine Research* 32:195–207.

Pickart, R.S., G.W.K. Moore, Chongyuan Mao, F. Bahr, C. Nobre, and T.J. Weingartner. In press. Circulation of Winter Water on the Chukchi Shelf in early summer. *Deep-Sea Research Part II*.

Pickart, R.S., L.J. Pratt, D.J. Torres, T.E. Whitledge, A.Y. Proshutinsky, K. Aagaard, T.A. Agnew, G.W.K. Moore, and H.J. Dail. 2010. Evolution and dynamics of the flow through Herald Canyon in the western Chukchi Sea. *Deep Sea Research Part II* 57(1–2):5–26, http://dx.doi.org/10.1016/j.dsr2.2009.08.002.

Pickart, R.S., M.A. Spall, G.W.K. Moore, T.J. Weingartner, R.A. Woodgate, K. Aagaard, and K. Shimada. 2011. Upwelling in the Alaskan Beaufort Sea: Atmospheric forcing and local versus non-local response. *Progress in Oceanography* 88:78–100, http://dx.doi.org/10.1016/j.pocean.2010.11.005.

Pickart, R.S., T.J. Weingartner, S. Zimmermann, D.J. Torres, and L.J. Pratt. 2005. Flow of winter-transformed water into the western Arctic. *Deep Sea Research Part II* 52:3,175–3,198, http://dx.doi.org/10.1016/j.dsr2.2005.10.009.

Pisareva, M.N., R.S. Pickart, M.A. Spall, C. Nobre, D.J. Torres, G.W.K. Moore, and T.E. Whitledge. 2015. Flow of Pacific water in the western Chukchi Sea: Results from the 2009 RUSALCA expedition. *Deep Sea Research Part II* 105:53–73, http://dx.doi.org/10.1016/j.dsr.2015.08.011.

Ravelo, A.M., B. Konar, J.H. Trefry, and J.M. Grebmeier. 2014. Epibenthic community variability in the northeastern Chukchi Sea. *Deep Sea Research Part II* 102:119–131, http://dx.doi.org/10.1016/j.dsr2.2013.07.017.

Reynolds, R.W., T.M. Smith, C. Liu, D.B. Chelton, K.S. Casey, and M.G. Schlax. 2007. Daily high-resolution-blended analyses for sea surface temperature. *Journal of Climate* 20:5,473–5,496, http://dx.doi.org/10.1175/2007JCLI1824.1.

Spall, M.A. 2007. Circulation and water mass transformation in a model of the Chukchi Sea. *Journal of Geophysical Research* 112, C05025, http://dx.doi.org/10.1029/2005JC003364.

Steele, M., R. Rebecca, and W. Ermold. 2001. PHC: A global ocean hydrography with a high-quality Arctic Ocean. *Journal of Climate* 14:2,079–2,087, http://dx.doi.org/10.1175/1520-0442(2001)014<2079:PAGOHW>2.0.CO;2.

Steele, M., J. Zhang, and W. Ermold. 2010. Mechanisms of summertime upper Arctic Ocean warming and the effect on sea ice melt. *Journal of Geophysical Research* 115, C11004, http://dx.doi.org/10.1029/2009JC005849.

Tang, X., W.K. Stewart, L. Vincent, H. Huang, M. Marra, S.M. Gallager, and C.S. Davis. 1998. Automatic plankton image recognition. *Artificial Intelligence Review* 12:177–199, http://dx.doi.org/10.1007/978-94-011-5048-4_9.

Timmermans, M.L., A. Proshutinsky, I. Ashik, A. Beszczynska-Moeller, E. Carmack, I. Frolov, R. Ingvaldsen, M. Itoh, J. Jackson, Y. Kawaguchi, and others. 2012. Ocean. *Arctic Report Card: Update for 2012*, http://www.arctic.noaa.gov/report12/ocean.html.

von Dassow, M. 2005. Flow and conduit formation in the external fluid-transport system of a suspension feeder. *Journal of Experimental Biology* 208:2,931–2,938, http://dx.doi.org/10.1242/jeb.01738.

Wang, J., K. Mizobata, X. Bai, H. Hu, M. Jin, Y. Yu, M. Ikeda, W. Johnson, W. Perie, and A. Fujisaki. 2014. A modeling study of coastal circulation and landfast ice in the nearshore Beaufort and Chukchi seas using CIOM. *Journal of Geophysical Research* 119:3,285–3,312, http://dx.doi.org/10.1002/2013JC009258.

Weingartner, T.J., K. Aagaard, R. Woodgate, S. Danielson, Y. Sasaki, and D. Cavalieri. 2005. Circulation on the north central Chukchi Sea shelf. *Deep Sea Research Part II* 52:3,150–3,174, http://dx.doi.org/10.1016/j.dsr2.2005.10.015.

Weingartner, T.J., D.J. Cavalieri, K. Aagaard, and Y. Sasaki. 1998. Circulation, dense water formation, and outflow on the Northeast Chukchi Shelf. *Journal of Geophysical Research* 103:7,647–7,661, http://dx.doi.org/10.1029/98JC00374.

Weingartner, T.J., S. Danielson, Y. Sasaki, V. Pavlov, and M. Kulakov. 1999. The Siberian Coastal Current: A wind and buoyancy-forced Arctic coastal current. *Journal of Geophysical Research* 104:29,697–29,713, http://dx.doi.org/10.1029/1999JC900161.

Weingartner, T., E. Dobbins, S. Danielson, P. Winsor, R. Potter, and H. Statscewich. 2013. Hydrographic variability over the northeastern Chukchi Sea shelf in summer-fall 2008–2010. *Continental Shelf Research* 67:5–22, http://dx.doi.org/10.1016/j.csr.2013.03.012.

Whitledge, T.E., S.C. Malloy, C.J. Patton, and C.D. Wirick. 1981. *Automated Nutrient Analysis in Seawater*. Brookhaven National Laboratory Technical Report BNL 51398.

Wildish, D., and D. Kristmanson. 2005. *Benthic Suspension Feeders and Flow*. Cambridge University Press, 424 pp.

Winsor, P., and D.C. Chapman. 2004. Pathways of Pacific water across the Chukchi Sea: A numerical model study. *Journal of Geophysical Research* 109, C03002, http://dx.doi.org/10.1029/2003JC001962.

Wlodarska-Kowalczuk, M., and T.H. Pearson. 2004. Soft-bottom macrobenthic faunal associations and factors affecting species distributions in an Arctic glacial fjord (Kongsfjord, Spitsbergen). *Polar Biology* 27:155–167, http://dx.doi.org/10.1007/s00300-003-0568-y.

Wood, K.R., J. Wang, S.A. Salo, and P.J. Stabeno. 2015. The climate of the Pacific Arctic during the first RUSALCA decade 2004–2013. *Oceanography* 28(3):24–35, http://dx.doi.org/10.5670/oceanog.2015.55.

Woodgate, R.A., K. Aagaard, and T.J. Weingartner. 2005. A year in the physical oceanography of the Chukchi Sea: Moored measurements from autumn 1990–1991. *Deep Sea Research Part II* 52:3,116–3,149, http://dx.doi.org/10.1016/j.dsr2.2005.10.016.

Woodgate, R.A., K.M. Stafford, and F.G. Prahl. 2015. A synthesis of year-round interdisciplinary mooring measurements in the Bering Strait (1990–2014) and the RUSALCA years (2004–2011). *Oceanography* 28(3):46–67, http://dx.doi.org/10.5670/oceanog.2015.57.

Woodgate, R.A., T.J. Weingartner, and R. Lindsay. 2012. Observed increases in Bering Strait oceanic fluxes from the Pacific to the Arctic from 2001 to 2011 and their impacts on the Arctic Ocean water column. *Geophysical Research Letters* 39, L24603, http://dx.doi.org/10.1029/2012GL054092.

Yun, M.S., T.E. Whitledge, M. Kong, and S.H. Lee. 2014. Low primary production in the Chukchi Sea shelf, 2009. *Continental Shelf Research* 76:1–11, http://dx.doi.org/10.1016/j.csr.2014.01.001.

Zhao, M., M.-L. Timmermans, S. Cole, R. Krishfield, A. Proshutinsky, and J. Toole. 2014. Characterizing the eddy field in the Arctic Ocean halocline. *Journal of Geophysical Research* 119:8,800–8,817, http://dx.doi.org/10.1002/2014JC010488.

ACKNOWLEDGMENTS

AUTHORS

Maria N. Pisareva (mnpisareva@gmail.com) is Junior Research Scientist and a PhD candidate at the P.P. Shirshov Institute of Oceanology, Moscow, Russia. **Robert S. Pickart** is Senior Scientist, Woods Hole Oceanographic Institution, Woods Hole, MA, USA. **Katrin Iken** is Professor, School of Fisheries and Ocean Sciences, University of Alaska Fairbanks, Fairbanks, AK, USA. **Elizaveta A. Ershova** is a joint PhD candidate at the Institute of Marine Science, University of Alaska Fairbanks, Fairbanks, AK, USA, and the P.P. Shirshov Institute of Oceanology, Moscow, Russia. **Jacqueline M. Grebmeier** is Research Professor, Chesapeake Biological Laboratory, University of Maryland Center for Environmental Science, Solomons, MD, USA. **Lee W. Cooper** is Research Professor, Chesapeake Biological Laboratory, University of Maryland Center for Environmental Science, Solomons, MD, USA. **Bodil A. Bluhm** is Affiliate Faculty, School of Fisheries and Ocean Sciences, University of Alaska Fairbanks, Fairbanks, AK, USA, and Professor, Department of Arctic and Marine Biology, UiT-The Arctic University of Norway, Tromsø, Norway. **Carolina Nobre** is Research Associate, Woods Hole Oceanographic Institution, Woods Hole, MA, USA. **Russell R. Hopcroft** is Professor, Institute of Marine Science, University of Alaska Fairbanks, Fairbanks, AK, USA. **Haoguo Hu** is Research Computer Specialist, School of Natural Resources and the Environment/Cooperative Institute for Limnology and Ecosystems Research, University of Michigan, Ann Arbor, MI, USA. **Jia Wang** is Research Ice Climatologist/Physical Oceanographer, National Oceanic and Atmospheric Administration, Great Lakes Environmental Research Laboratory, Ann Arbor, MI, USA. **Carin J. Ashjian** is Senior Scientist, Woods Hole Oceanographic Institution, Woods Hole, MA, USA. **Ksenia N. Kosobokova** is Leading Scientist, P.P. Shirshov Institute of Oceanography, Moscow, Russia. **Terry E. Whitledge** is Director and Professor, Institute of Marine Science, University of Alaska Fairbanks, Fairbanks, AK, USA.

ARTICLE CITATION